Rare Met. (2022) 41(6):1921–1932
https://doi.org/10.1007/s12598-021-01943-6

RARE METALS

ORIGINAL ARTICLE

Tribocorrosion behavior of antibacterial Ti–Cu sintered alloys in simulated biological environments

Jia-Qi Zhang, Shuang Cao, Ying Liu, Mian-Mian Bao, Jing Ren, Sheng-Yi Li, Er-Lin Zhang, Jian-Jie Wang*

Received: 30 July 2021 / Revised: 19 September 2021 / Accepted: 13 October 2021 / Published online: 14 March 2022

Abstract Ti–Cu alloys have strong antibacterial properties, high strength and excellent corrosion resistance, which might be used in orthopedic and dental implants. In this paper, the tribocorrosion behaviors of Ti–Cu alloy with different Cu contents were investigated in four simulated biological environments compared with cp-Ti. The results showed that Ti–Cu sintered alloy exhibited higher corrosion resistance, lower coefficient friction and wear loss than cp-Ti in all tested solutions due to the formation of fine and homogeneously distributed Ti_2Cu phase, especially in solution with lower F ion and pH. High Cu content and extrusion process improved the corrosion resistance and the wear resistance because of high Ti_2Cu phase fraction and fine grain size. However, aggressive solution, such as the solution with lower F ion and pH, accelerated wear in comparison with other solutions for cp-Ti and Ti–Cu sintered alloys. Scanning electron microscope (SEM) surface morphology demonstrated that the wear mechanism of cp-Ti during tribocorrosion process was mainly abrasive wear and adhesive wear while that of Ti–Cu alloy was abrasive wear. In summary, Ti–Cu sintered alloys showed much better tribocorrosion property than cp-Ti, which shows great potential application in condition for wear and corrosion resistance.

Keywords Ti–Cu alloys; Tribocorrosion; Corrosion; Wear; In vitro; Antibacterial metal alloy

1 Introduction

Titanium and titanium alloys are applied to lots of industries because of their outstanding corrosion function and mechanical resistance [1]. Currently, titanium and its alloys have become more popular metal implantable biomaterials due to their more excellent bio-compatibility than stainless steels and cobalt alloys [2–4]. But some obstacles still need to be overcome when titanium alloys are successfully used in dentures or artificial joints.

One disadvantage of pure titanium is the lack of antibacterial property, which might lead to infection or inflammation in clinic application [5–8], even implantation failure [9, 10]. Antibacterial coating has been developed to reducing the infection and inflammation. Zhao et al. [11] reported that the coatings delivering nitrogen monoxide (NO), anti-adhesion coatings and the paint coat including nanobiotic organic/inorganic germifuge on titanium prevented early postsurgical infection caused by surgical contamination. Liu et al. showed an antibacterial coating on the surface of titanium alloy by micro-arc oxidation (MAO) and further nitrogen plasma immersion ion implantation (N-PIII), effectively improving the antibacterial properties of the titanium alloy [12]. Wu et al. developed a controlled drug release polymer coating on titanium, which improves both the osteoblasts adhesion and

Jia-Qi Zhang and Shuang Cao have contributed equally to this work.

J.-Q. Zhang, J.-J. Wang*
Departments of Immunology, College of Basic Medicine, Jiamusi University, Jiamusi 154007, China
e-mail: jmsdxjianjie@163.com

S. Cao, Y. Liu, M.-M. Bao, J. Ren, S.-Y. Li, E.-L. Zhang
Key Laboratory for Anisotropy and Texture of Materials, School of Materials Science and Engineering, Education Ministry of China, Northeastern University, Shenyang 110819, China

E.-L. Zhang
Research Center for Metallic Wires, Northeastern University, Shenyang 110819, China

antibacterial activity [13]. Jin et al. [14] researched the antibacterial Ti–Cu coating on 316L stainless steel, which can kill more than 99.9% *E. coli* within 12-h contact attributed to the release of Cu ion. Similar experiments also found that both Ti–Cu films and Ti–Cu–N coatings had strong antibacterial properties compared with cp-Ti [15].

Another disadvantage of pure titanium is its poor tribological characteristics [16], which may lead to aseptic loosening and even the osteolysis due to the joint wear after the implantation and limit its long-term application [17]. Over the past decades, more emphases have been focused on studying the tribological corrosion behaviors of metal materials with the combined action of chemical, mechanics and electrochemical, especially materials used as implants. Pina et al. [18] researched the microstructure, electrochemistry and abrasive wear of Ti–*x*Cu and found Ti–Cu alloy with a high hardness exhibited low wear loss in saliva solution. But, the corrosion resistance in the worse environment such as low pH or fluorine remains to be studied.

The passive film on the contact surface would be damaged or even completely fall off because of tribocorrosion, thus speeding up the wear rate of the contact surface and leading to accelerated wear corrosion and vice versa. For the most parts, the damage of material is mainly caused by tribocorrosion compared with summation of mechanical wear and static corrosion [19–21]. It is generally believed that there is cooperative reaction between corrosion and wear [18, 22]. Previous studies have concentrated on the understanding of complex phenomena, including determining the cooperative effect between corrosion, wear and quantifying the cooperative part through mathematical models [23, 24].

In our previous studies [25–30], compared with cp-Ti, Ti–Cu sintered alloys have exhibited superior antibacterial performance, higher hardness and yield strength and more excellent corrosion resistance in 0.9% NaCl solution. Other studies have also authenticated that the Cu-bearing Ti alloy has strong antibacterial function [31]. The results show that Ti–Cu sintered alloy combined powerful antibacterial ability and high hardness and yield strength, which could reduce the infection effectively and provide good tribological wear properties for joints or dental replacement application.

Tribocorrosion phenomenon of a metal alloy is normally affected by the mechanical properties of metal alloy, but it is more easily affected by the properties of a simulated body fluid (SBF). In this paper, four typical SBFs, Hank's solution, Saliva-pH 6.8 solution, Saliva-pH 6.8 + 0.2F (Saliva-pH 6.8 + 0.2 wt% NaF) solution and Saliva-pH 3.5 solution, were selected to simulate different biological environments, including bone implant and oral environment. The tribocorrosion phenomenon of the antimicrobial Ti–Cu alloy in above SBFs was studied for the first time as we know by means of electrochemical workstation and tribometer, aiming at evaluating the potential application of antibacterial Ti–Cu alloys in different environments. Preliminary results demonstrated that Ti–Cu sintered alloy showed better corrosion resistance and lower wear rate in all test solutions than cp-Ti, especially in F ion containing and low pH solutions, which displays the good tribocorrosion resistance of Ti–Cu sintered alloy.

2 Experimental

2.1 Preparation of sample

Ti–Cu sintered alloys with 5 wt% and 10 wt% Cu were prepared by a method of powder metallurgy, and designated as Ti–5Cu(S) and Ti–10Cu(S) alloy, respectively. More details can be found in Ref. [32]. After this, the sintered alloys were extruded into 16-mm-diameter bars at an extrusion rate of 10 $mm{\cdot}s^{-1}$ at 800 °C and designated as Ti–5Cu(E) alloys and Ti–10Cu(E) alloys, respectively. Besides, for comparison, industrial pure titanium bar was used as a contrast group. The samples were ground using a series of SiC sand papers from 120 to 2000 grit and polished with 1 μm polishing paste. After that, the surfaces were cleaned ultrasonically for 5 min in ethanol and ultrapure water, respectively, and then dried with warm air. The surface roughness of samples was about 0.07–0.08 μm, and no difference among the samples was observed.

2.2 Microstructure and hardness

The specimens used for microstructure observation were prepared according to the conventional metallographic methods, including grinding and mechanical polishing. X-ray diffraction (XRD, Smart Lab Rigaku) was used to identify the phase with the accelerating voltage of 40 kV, the current of 40 mA and the scan step of 0.02. The sample was etched by Keller's solution, and the microstructure was analyzed by scanning electron microscopy (SEM, JSM-6510A) with equipped energy-dispersive X-ray spectroscopy (EDS). Microhardness was measured by Vickers hardness tester (401MVDTM Huayin, China). The test load was 2 N, and the duration time was 10 s. Five different samples were randomly selected, and the result was the average value of five samples.

2.3 Tribocorrosion experiments

Tribocorrosion behavior of the samples was estimated by a tribo-electrochemical technique with a Si_3N_4 ball (Φ = 4 mm) as counter material. The sample was tested

with a normal load of 2 N, the stroke length was 100 m and the frequency was 150 r·min^{-1}. The electrochemical workstation with a three-electrode cell system was employed to record the variation in open current potential (OCP). Before sliding, specimens were immersed in the corresponding SBF for 600 s to obtain a stable potential. Once the sliding started, the OCP was recorded until 3600 s, and then dynamic polarization behavior curve was measured. After sliding, the OCP was recorded for another 600 s continuously. Four kinds of SBFs as listed in Table 1 were used to simulate different kinds of body environment.

The change of friction factor with sliding was checked by sensor and recorded by computer. Then, worn surface was carefully cleaned with acetone, alcohol and distilled water. After that, the cross-sectional profiles of the wear tracks and the wear rates of the titanium alloys were measured and calculated by a MitutoyoSurftest SJ-301. The morphology of the worn surface was investigated under SEM. At least two identical samples were test under each test condition for obtaining good reproducibility.

3 Results

3.1 Microstructure and hardness

Figure 1 shows microstructure of Ti–Cu(S) and Ti–Cu(E). Previous study has reported that only the diffraction peaks of Ti_2Cu phase as well as Ti matrix were detected by XRD, which demonstrated in combination with EDS results that only Ti_2Cu phase was synthesized during the sintering process and the following extrusion [33]. In these alloys, numerous small Ti_2Cu particles were synthesized. With the increase in Cu content, the volume fraction of Ti_2Cu grains increased significantly. The microstructure of Ti–Cu(E) in Fig. 1b, d displayed that the extrusion processing refined Ti_2Cu particles significantly in Ti–5Cu and Ti–10Cu alloys. Because of the formation of fine Ti_2Cu particle in Ti–5Cu(S) and Ti–10Cu(S) alloys, the hardness of Ti-Cu(S) alloys increased sharply from HV 160 of cp-Ti to HV 354 of Ti–5Cu(S) and HV 420 of Ti–10Cu(S), indicating that the increase in Ti_2Cu particle fraction increased the hardness. Although extrusion processing enhanced the hardness of Ti–5Cu sintered alloy, it had no effect on the hardness of Ti–10Cu alloy.

Table 1 Chemical composition of stimulated biological mediums (g·L^{-1})

Solution	Hank's	Saliva	Saliva + 0.2F	Saliva-pH 3.5
Lactic acid	–	10	10	10
NaCl	8.00	5.85	5.85	5.85
NaF	–	–	2	–
KCl	0.40			
$CaCl_2·H_2O$	0.14	–	–	–
$NaHCO_3$	0.35	–	–	–
$MgSO_4·7H_2O$	0.06	–	–	–
$MgCl_2·6H_2O$	0.10	–	–	–
Na_2HPO_4	0.06	–	–	–
KH_2PO_4	0.06	–	–	–
Glucose	1.00	–	–	–
pH	7.4	6.8	6.8	3.5

3.2 OCP and Tafel curves with sliding

Figure 2a–e shows OCP curves of cp-Ti, and Ti–Cu samples with and without sliding in four SBFs, respectively. For all samples, at the first 600 s (before sliding), with the extension of the soaking time, the potential gradually increased, showing that a passive film was gradually produced on the sample. Once sliding began, a sharp decline in the potential was observed, illustrating that the passive film was damaged due to the sudden sliding; as a result, the corrosion was accelerated. During the sliding, the potential stabled at or fluctuated around a very low value (named dynamic open circuit potential, DOCP, thereafter) depending on the fluids and material. The fluctuation was mainly due to the electrochemical re-passivation while the mechanical damage and wear of the passivation film occur. After the sliding, the potential rose immediately to the initial potential level, indicating that the wear trace was re-passivated.

Figure 2a2–e2 shows dynamic polarization behavior curves of Ti–Cu alloys in different SBFs with sliding. Tafel curves without sliding are also shown for comparison. It clearly reports that the polarization region of Tafel curves after the sliding moved toward the high value direction in the current density (i_{corr}) and the negative direction in the potential in all cases, indicating that the sliding process accelerated the corrosion vastly.

Figure 3a depicts DOCP of titanium alloys in SBFs obtained from the above OCP curves. The DOCP of Ti–Cu(s) alloys was slightly higher than that of cp-Ti in all SBFs. Different solutions also led to the change of DOCP. In both Saliva + 0.2F solution and Saliva-pH 3.5 solution, there was a vastly decrease in DOCP between cp-Ti and Ti–Cu alloys, indicating that F^- and pH 3.5 have a negative effect on the corrosion potential.

Figure 3b shows the corrosion current density of titanium alloys after the sliding wear in different solutions. In Saliva + 0.2F and Saliva-pH 3.5 solutions, the corrosion current density of all titanium alloys was obviously higher than those in Hank's and Saliva solutions, indicating that F ion and low pH have a negative effect on material

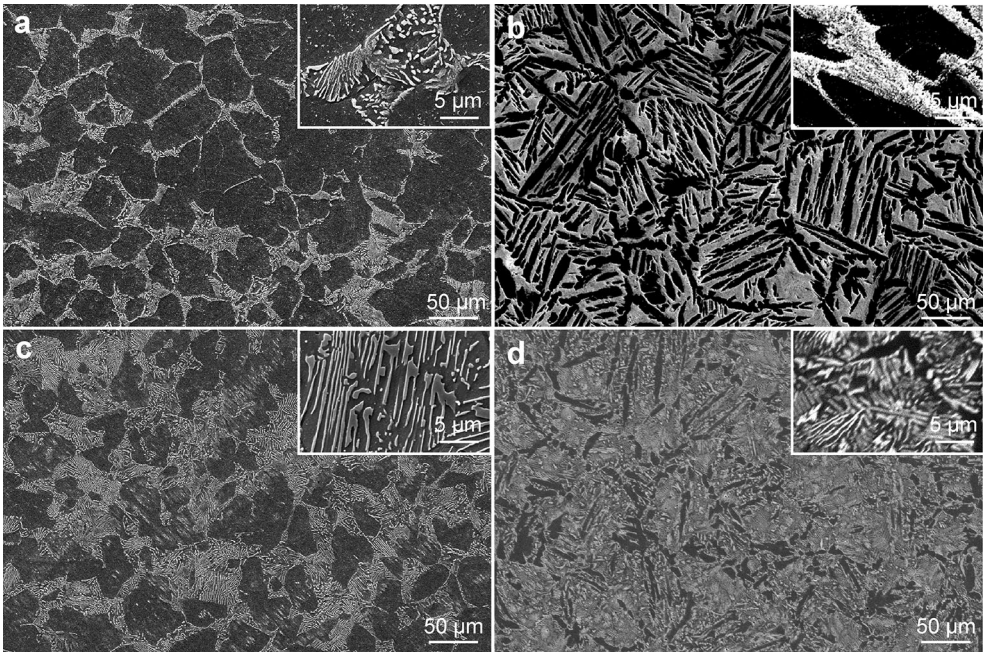

Fig. 1 Microstructure of Ti–Cu sintered alloys: **a** Ti–5Cu(S), **b** Ti–5Cu(E), **c** Ti–10Cu(S) and **d** Ti–10Cu(E)

corrosion. Besides, the corrosion current density of Ti alloy was decreased slightly in all test solutions by the addition of copper and the extrusion process, especially in Saliva + 0.2F and Saliva + pH 3.5 solutions, displaying that the corrosion rate of Ti–Cu alloys was slower than that of cp-Ti.

3.3 Friction

Figure 4 illustrates the fluctuation of the friction factor of Ti alloy in SBFs. Friction coefficient increased at first and then decreased, and finally stabilized at 0.3–0.4. Probably in the early wear, high surface hardness and smooth surface made the friction coefficient low.

As the wear leveling surface was damaged, the surface roughness increased, and then the friction coefficient increased. Then, with the accumulation of the peeling particles, debris would play a solid lubricating effect. When the debris generation speed and the overflow speed from the contact surface achieved dynamic equilibrium, the friction coefficient changed and entered a relatively stable period.

Figure 4f shows that the friction coefficient of cp-Ti in different SBFs changed significantly, but the friction coefficient of Ti–Cu alloy varied slightly, indicating that SBFs acted little upon the friction coefficient of Ti–Cu alloy, even in F ion containing and low pH solutions, although they played a vital part on the corrosion behavior. In addition, the friction coefficients of cp-Ti in all wear conditions were obviously higher than those of Ti–Cu samples. The addition of Ti_2Cu in Ti–Cu alloy could significantly increase the hardness and the compressive yield strength of Ti–Cu alloy and the corrosion resistance of Ti–Cu. During the tribocorrosion, the high hardness and the compressive yield strength would resist the compressive deformation, therefore reducing the contact interface between the Ti–Cu sample and Si_3N_4 ball, thus reducing the coefficient. On the other hand, the good corrosion resistance also reduced the corrosion rate and kept the interface smoother, thus reducing the coefficient. Finally, the hard Ti_2Cu particle reduced the friction coefficient.

Figure 5 presents the wear rates of cp-Ti and Ti–Cu alloys in SBFs. In all cases, the wear rate of Ti–Cu alloys was much lower than that of cp-Ti, indicating that the wear resistance of Ti–Cu alloys was improved obviously by copper element alloying. Also, the extruded alloys illustrated a slightly slower wear rate than the corresponding sintered alloys. It can also be found that the changes in the solutions also had an effect on the wear resistance. A much faster wear rate was observed for all alloys in Saliva + 0.2F solution and Saliva-pH 3.5 solution than that in Hank's solution, showing the strong aggressive ability of the two solutions.

3.4 Surface morphology of worn track

Figure 6 shows surface morphology of different samples inspected by SEM. Figure 6a1–a4 represents the worn surface morphology of cp-Ti samples in SBFs. According to Fig. 6a1, a2, in Hank's and Saliva solution, there mainly

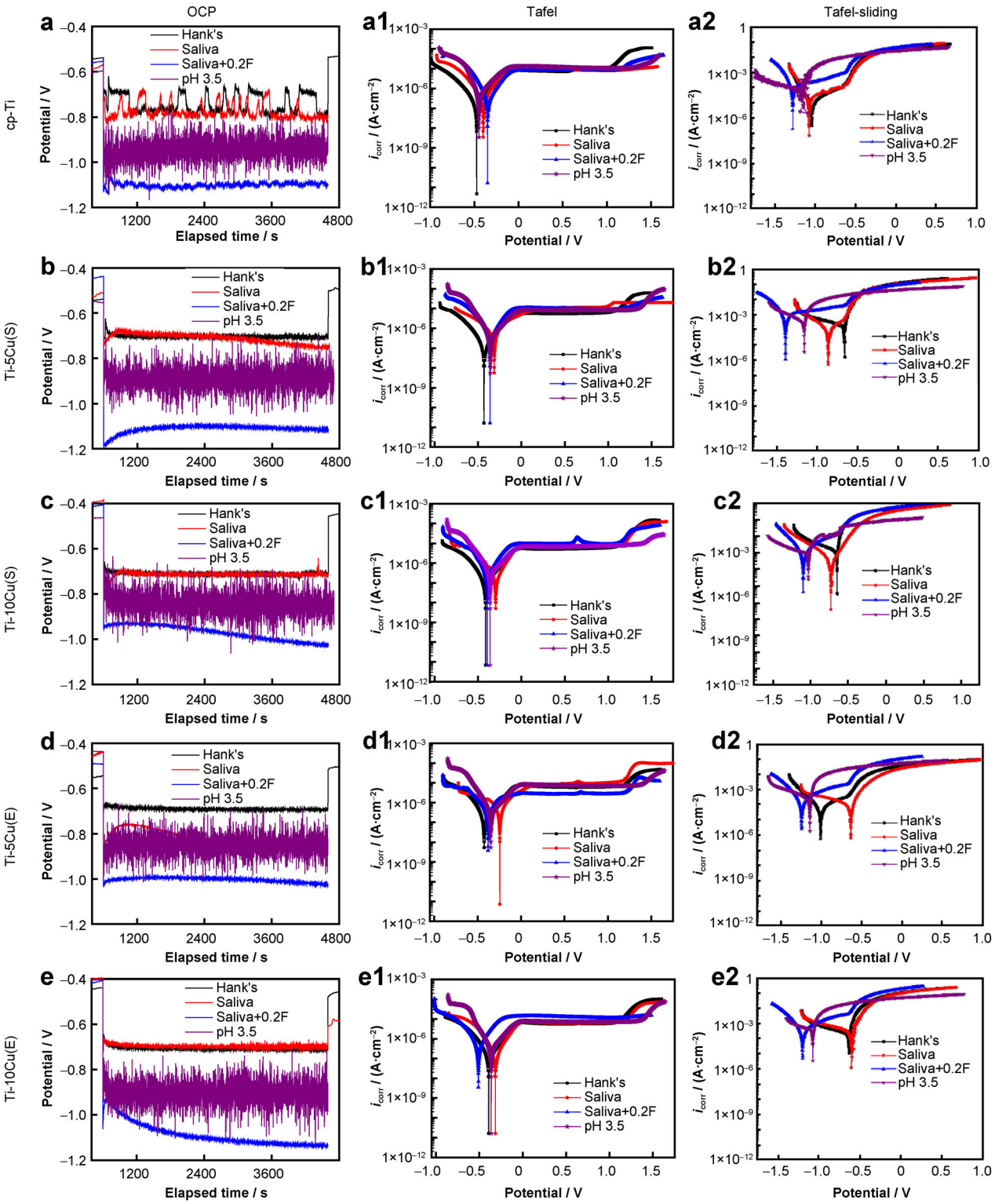

Fig. 2 OCP and dynamic polarization behavior of Ti–Cu alloys in solutions with and without sliding: **a**–**a2** cp-Ti, **b**–**b2** Ti–5Cu(S), **c**–**c2** Ti–10Cu(S), **d**–**d2** Ti–5Cu(E), and **e**–**e2** Ti–10Cu(E)

appeared some furrows along the sliding direction and no obvious adhesion appeared on the surface of cp-Ti. In Saliva + 0.2F solution and Saliva-pH 3.5 solution, as shown in Fig. 6a3, a4, not only furrows but also wears debris were found on the worn surface. In Saliva-pH 3.5 solution, clear micro-cracks and fatigue-separated layers

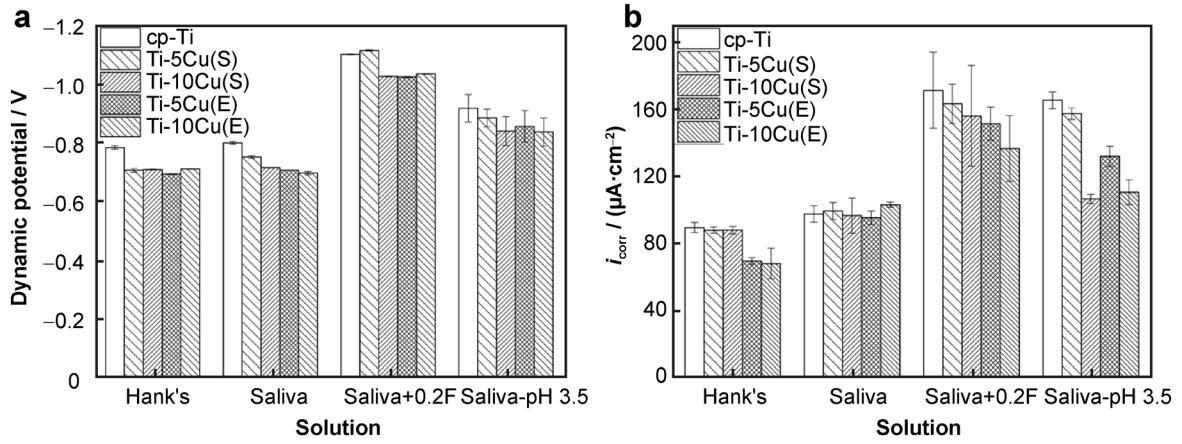

Fig. 3 Dynamic open circuit potential (DOCP) during sliding and corrosion current density after sliding of cp-Ti and Ti–Cu alloys in SBFs: **a** DOCP and **b** i_{corr}

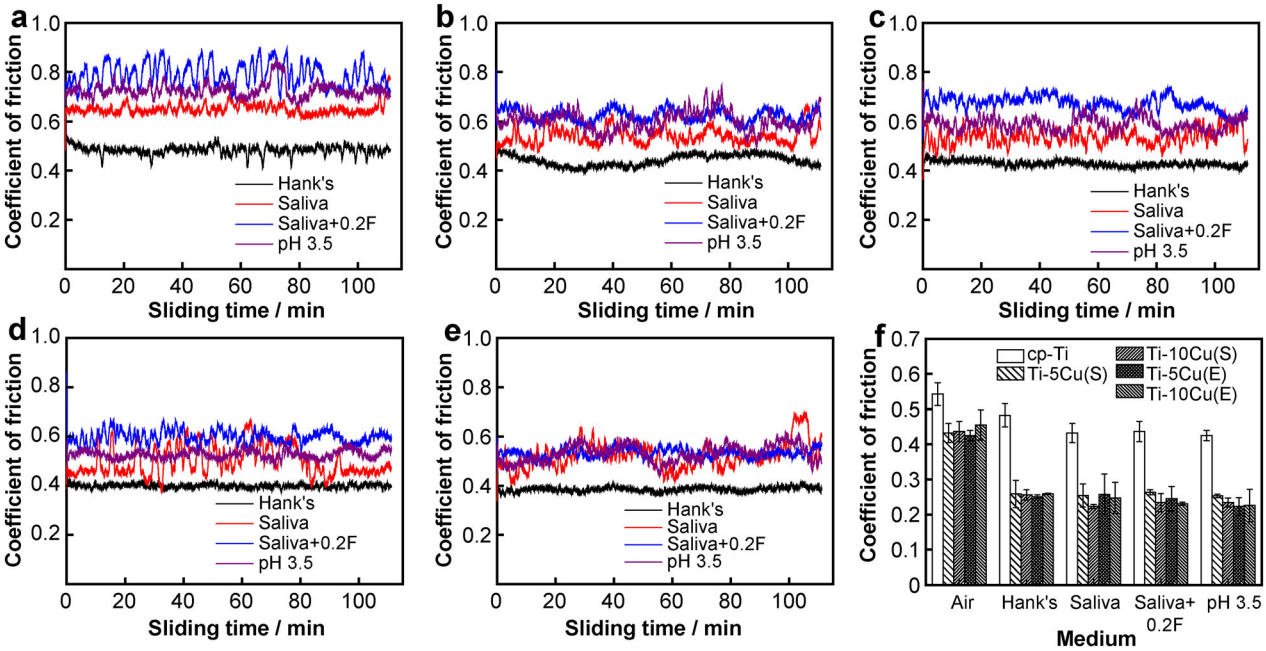

Fig. 4 Coefficient of friction of Ti–Cu alloys in SBFs: **a** cp-Ti, **b** Ti–5Cu(S), **c** Ti–10Cu(S), **d** Ti–5Cu(E), and **e** Ti–10Cu(E); **f** coefficient of friction of cp-Ti and Ti–Cu alloys

were found on the surface, indicating the wear was serious particularly.

Figure 6b1–b4 and c1–c4 shows the worn surface morphology of Ti–5Cu(S) and Ti–10Cu(S) in four SBFs, respectively. Compared with the worn surface of cp-Ti under corresponding conditions, it can be seen that the surface was flatter, and no notable adhesion and debris were observed, displaying that the wear resistance was improved slightly by adding Cu in a dose dependent way. In Hank's solution or Saliva solution, the furrow was more obvious on the worn surface, displaying that the main wear form was abrasive wear. Obvious furrow and serious peeling were observed on the worn surfaces in Saliva + 0.2F solution and Saliva-pH 3.5 solution, a typical abrasive wear and adhesive wear, showing strong aggressive ability of these two solutions.

The worn morphologies of Ti–5Cu(E) and Ti–10Cu(E) are exhibited in Fig. 6d1–d4 and e1–e4, respectively. It can be observed that in Hank's and Saliva solution, the worn surface was relatively smooth and the furrow was shallow. In Saliva + 0.2F solution and Saliva-pH 3.5 solution, the wear surface had a slight peeling besides shallow wear grooves. The results showed that the extrusion treatment could enhance the wear resistance of Ti–Cu alloys.

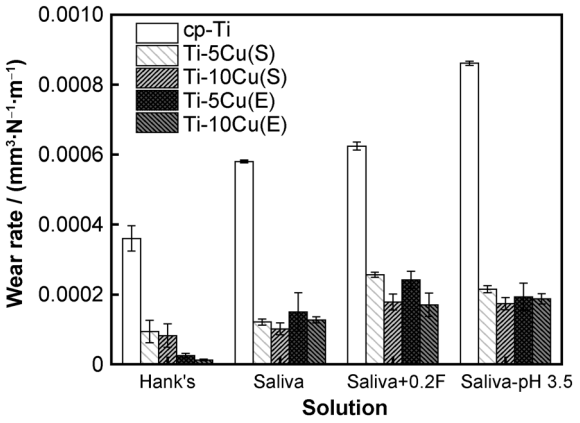

Fig. 5 Wear rates of different samples in different mediums

Figure 7 shows high magnification images of the worn surfaces in Saliva-pH 3.5 solution which has a strong aggressive effect on titanium and titanium copper alloys. On the cp-Ti surface (Fig. 7a), there were some obvious cracks due to the low hardness, while on the surface of Ti–Cu alloys (Fig. 7b–e), the same tendency was also observed. On the Ti–5Cu(S) surface (Fig. 7b), the cracks diminished, but some debris appeared. On the surfaces of Ti–10Cu(S) and Ti–5Cu(E), the worn surface become flatter and only visible furrows along the sliding direction could be seen on the surface of Ti–10Cu(E).

4 Discussion

Taking into account the complexity of the human biological environment, titanium alloy used as a biological material will subject to corrosion and wear, which will accelerate the destruction of materials [1, 34]. It was reported that antibacterial Ti–Cu alloys were produced by powder metallurgy [25]. Moreover, the presence of Ti_2Cu increased the hardness and corrosion resistance in 0.15 mol·L^{-1} NaCl solution [35]. Later study [26] found that the hardness and compressive yield strength of titanium-copper alloys and the corrosion resistance in 0.9% NaCl solution were significantly enhanced by hot extrusion, mainly due to grain refinement and fine Ti_2Cu. The compressive yield strength of Ti–Cu sintered alloys has been reported in our previous study, as listed in Table 2. Cp-Ti showed a very good ductility but low yield strength, and no break was observed even at a compressive stain of 50%. A yield strength of as high as 1050 MPa and a compressive strength of about 1800 MPa were observed for both Ti–5Cu(S) and Ti–10Cu(S) alloys, but the failure strain was only about 20%. The extruded Ti–Cu alloys displayed a higher compressive yield strength than the sintered alloy and even high compressive strength. No break was found under the maximum load, corresponding to a stain of 18.51% [33].

Microstructure in Fig. 1 clearly shows that Ti_2Cu intermetallic particles were synthesized in Ti–Cu alloy due to solid reaction during powder metallurgy processing. Five different samples have different Cu contents and materials processing process. High-Cu content would lead to high volume fraction of Ti_2Cu particles, which results in high hardness. Extrusion process also refined the microstructure, as shown in Fig. 1, which would also change the hardness.

Results in Fig. 2 have shown that the corrosion resistance of both cp-Ti and Ti–Cu alloys was negatively affected by F ion and pH value. Reclaru et al. [36] reported that F ion might be the most aggressive to the protection of titanium and its alloys. Lindholm-Sethson and Ardlin [37] also revealed the negative effect of low pH and fluoride. Moreover, the experimental result also showed that the addition of copper significantly decreased the corrosion current density and increased the corrosion resistance of titanium alloy in SBFs including Saliva + 0.2F and Saliva-pH 3.5 solutions in a content dependent way [37]. Similar results were also reported on Ti–Cu alloys under a different copper content [18]. The result suggested that the volume fraction of Ti_2Cu phase increased with the addition of copper [27]. In spite of a galvanic couple between Ti_2Cu intermetallic and the Ti matrix, it is suggested that fine microstructure could provide an "encapsulation effect" to change the cathode/anode area ratio between all phases to minimize the couple effect and increase the corrosion resistance [35, 38]. In addition, the grain size was refined and the microstructure of the alloy was optimized after the extrusion deformation treatment. In consequence, the corrosion resistance of the titanium alloy was increased by the uniform distribution of intermetallic.

In Figs. 2 and 3, the corrosion potential during the sliding process was much negative and the corrosion current density was much higher than the values without sliding, demonstrating that wear seriously accelerates the corrosion of titanium alloys. On the one hand, the wear resulted in the destruction of passivated film that was originally produced on the sample surface, and a fresh surface was constantly exposed to the solution, resulting in a decrease in the tribocorrosion resistance of the alloy. On the other hand, wear caused plastic trans-shape of wear marks, increased the densities of point defects, cracks and dislocations, making the surface more active, leading to the higher corrosion rate [39]. In addition, by comparing the corrosion current densities between cp-Ti and Ti-Cu(E) alloys during sliding, it will be deduced that the addition of copper and the deformation process enhanced the tribocorrosion resistance.

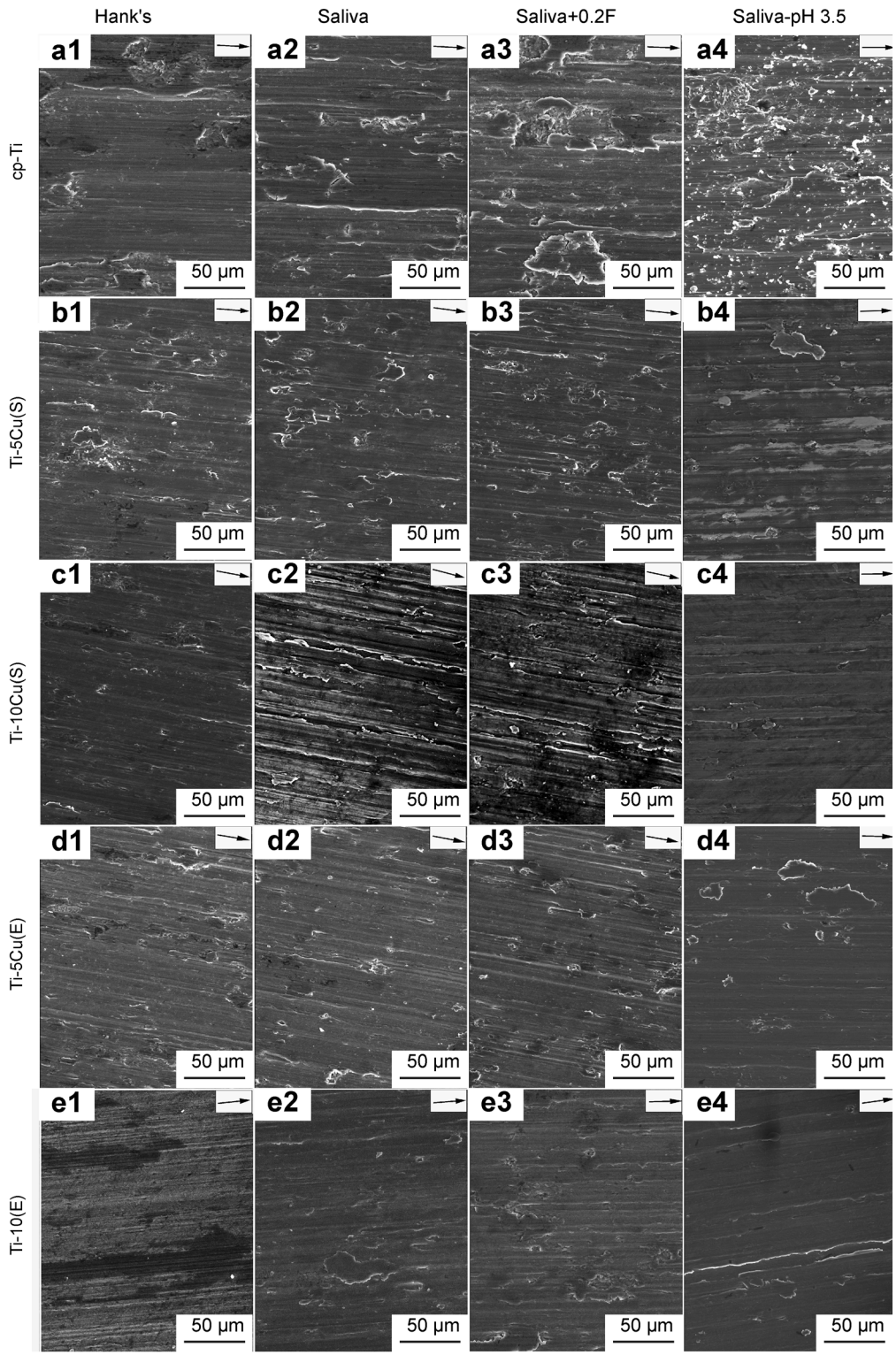

Fig. 6 SEM surface morphologies of wear scars on different samples in different SBFs: **a1**–**a4** cp-Ti, **b1**–**b4** Ti–5Cu(S), **c1**–**c4** Ti–10Cu(S), **d1**–**d4** Ti–5Cu(E) and **e1**–**e4** Ti–10Cu(E)

Different SBFs have different corrosion capacities and will have different corrosive effects on the material. Severe corrosion will increase the roughness of the material surface, and therefore, the coefficient of friction will be different. Liu and Zhang [40] showed that Ti–10Cu alloy exhibits high corrosion rate in Saliva pH 3.5 solution and

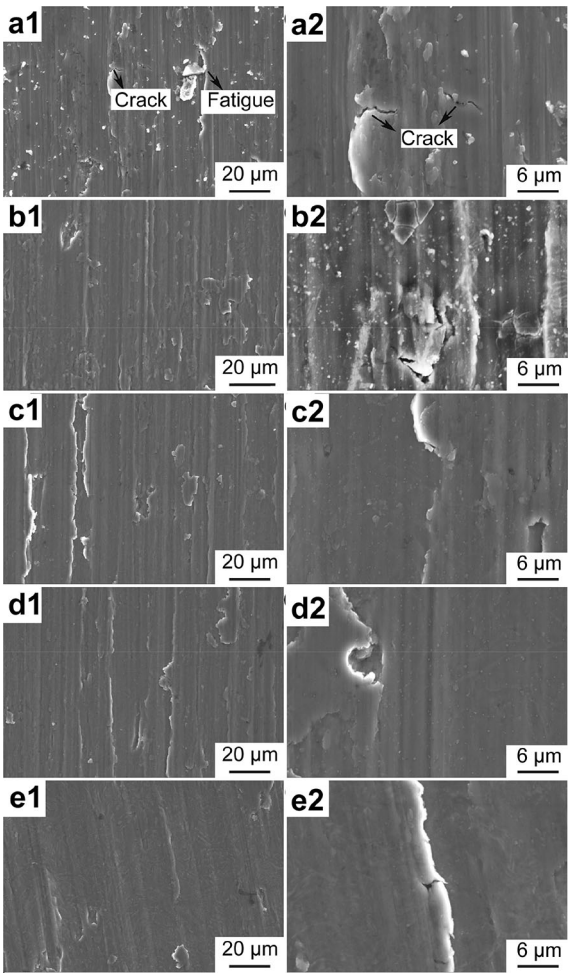

Fig. 7 High magnification SEM images of wear scars on different samples in Saliva-pH 3.5 solution: **a1**, **a2** cp-Ti; **b1**, **b2** Ti–5Cu(S); **c1**, **c2** Ti–10Cu(S); **d1**, **d2** Ti–5Cu(E); **e1**, **e2** Ti–10Cu(E)

Saliva pH 6.8 + 0.2F wt% NaF solution, but low corrosion rate in Hank's, Tyrode's and Saliva pH 6.8 solutions. During the sliding in SBFs, the corrosion potential dropped sharply at the beginning, illustrating that the passivated film was broken or fell off due to wear and causing bare surfaces exposed to electrolyte. After a short time, the potential increased and stabled for a short time again, illustrating that passive film was reformed on the surface but destroyed again after a short time. The fluctuation characteristic basically depends on the balance between destruction and re-passivation of the worn surface [41]. A higher fluctuation frequency was found in Saliva-pH 3.5 solution than in Hank's and Saliva solution. All these displayed that the destruction and re-passivation rate was faster in Saliva-pH 3.5. Saliva-pH 3.5 solution has strong aggressive ability and a strong oxidation ability, which makes Ti–Cu alloy surface easy to passivate previous film.

The combination of wear and corrosion can destroy or remove the passivated film formed on the surface of metal alloy. Thus, in the sliding process, the surface of the passivation film was rapidly formed and destroyed immediately, resulting in obvious and high frequency fluctuation. However, no fluctuation was found in Saliva + 0.2F solution, showing that no passivation film was formed on the sample surface during sliding because of the high aggressive property of Saliva + 0.2F solution. For Ti–Cu alloys, both the sintered and the extruded alloys, no obvious fluctuation in OCP curves was observed in Hank's and Saliva solutions, showing that no passivation film was formed in the sliding process. Owing to the structure difference between cp-Ti and Ti–Cu alloys, it was proposed that the presence of fine Ti_2Cu phase prevented the formation of a passive film or a continuous passive film, as illustrated in Fig. 8.

The ultimate wear mechanism and behavior of experimental material may be affected by testing parameters and movement patterns, including lubricating medium [39], imposed loading and sliding velocity [41, 42] and counterface material [38]. It was reported by Wimmer et al. [43] that abrasion, adhesion, tribo-chemical reactions, and surface fatigue were the four main factors governing the wear behavior of metal hip joint axle bearings. The flatter worn surface of Ti–Cu alloy in Fig. 6 displays that the hardness of the material itself also plays a very important part through the wear loss. Taking the great difference in hardness between Si_3N_4 ball (about HV 1500) and Ti alloy (HV 150–HV 300) into account, it can be deduced that the main removal force of material should be plowing. The wear mechanism of cp-Ti with relatively low hardness should be mainly an adhesive wear with abrasive wear. The addition of copper element, leading to the precipitation of hard Ti_2Cu phase, increased the hardness and wear quality

Table 2 Mechanical properties of cp-Ti and Ti–Cu alloys [33]

Alloys (condition)	Compressive yield strength/ MPa	Hardness (HV)	Compressive strength/ MPa
Ti–5Cu(S)	1050	350	1700
Ti–5Cu(E)	1267	405	> 2000
Ti–10Cu(S)	1050	425	1800
Ti–10Cu(E)	1325	425	> 2000

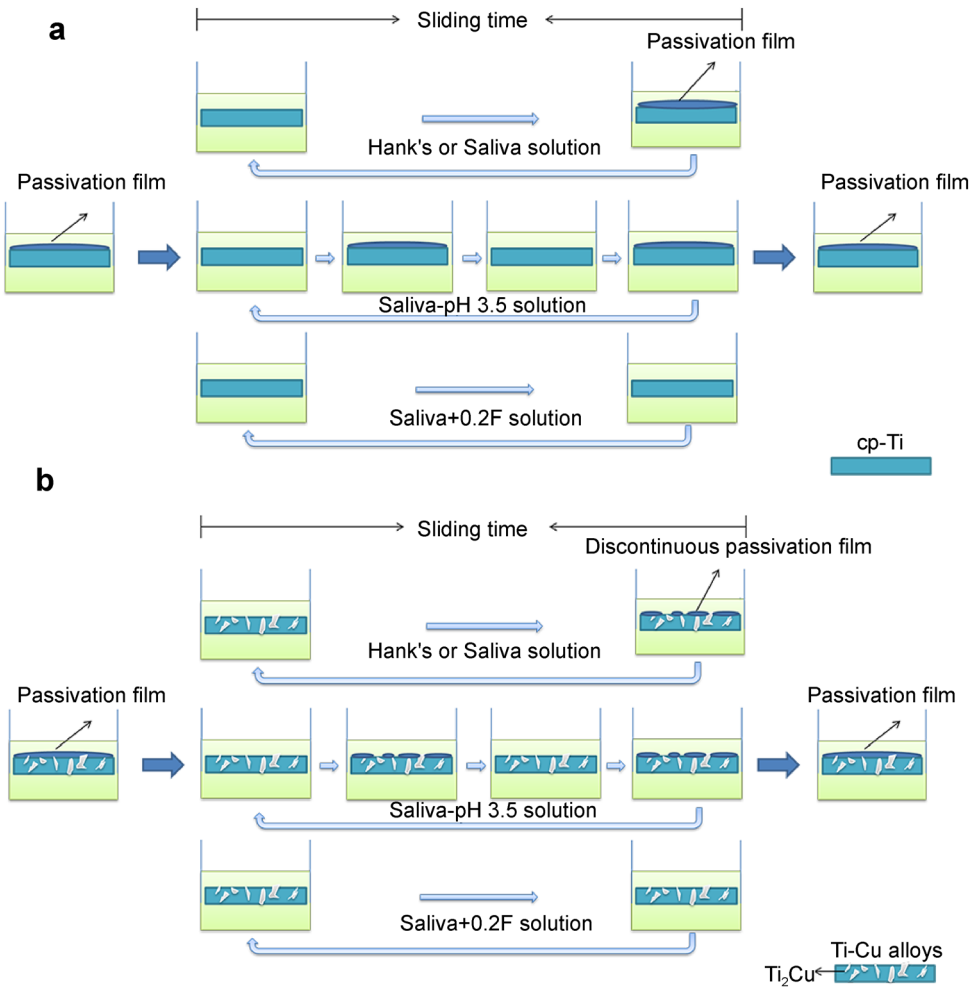

Fig. 8 Model of Ti and its alloys during tribocorrosion process: **a** cp-Ti and **b** Ti–Cu alloys

of materials. Therefore, abrasive wear was the main wear mechanism of Ti–Cu alloy.

When the samples were worn in Hank's and Saliva solutions, the wear surface, including that of cp-Ti and Ti–Cu alloys, was smooth. But in Saliva + 0.2F or Saliva-pH 3.5, which has a strong corrosive ability, the surface was worn seriously, even the appearance of cracks, showing that F^- and low pH have negative effects on wears and can accelerate wear.

Tribocorrosion process is a low cycle fatigue process, which including two stages of crack initiation and propagation. Moreover, the plastic deformation will cause high-density point defects and dislocations at the crack tip. Ti_2Cu in Ti–Cu alloy can reduce the wear degree of the alloy surface, and the surface cracks can be reduced due to the existence of Cu element. In Fig. 7, the cracks on the surface of cp-Ti were more obvious than those on the surface of Ti–Cu alloys.

Previous studies have indicated that Ti–Cu sintered alloys achieved good antimicrobial function and high mechanical properties. The results obtained in this study have shown that Ti alloys with copper addition had better corrosion resistance and wear resistance, while the copper improved the ability to confront comprehensive reaction in different SBFs. All the results strongly suggested that antibacterial Ti–Cu alloy have excellent biomedical application prospect in future.

However, it has to be pointed out that the wear accelerated the corrosion reaction, which in turn increased the Cu ion release and might cause cytotoxicity. Previous study has indicated that the maximum corrosion current density among the above four Ti–Cu alloys was 175 $nA{\cdot}cm^{-2}$ from Ti–5Cu(S) alloy, corresponding to a Cu release concentration of 47.1 $\mu g{\cdot}L^{-1}{\cdot}day^{-1}$ [33]. If we assume that the Cu ion release concentration in the static condition has the same relationship with the corrosion current density in the tribocorrosion condition, the highest Cu ion release concentration in this study would be about 43 $mg{\cdot}L^{-1}{\cdot}day^{-1}$. On the other hand, it has been reported that the minimum inhibition concentration of Cu ion against mesenchymal

stem cells (MSCs) was about 5×10^{-4} mol·L^{-1}, corresponding to 32 mg·L^{-1} [29]. Based on the above results, the Cu ion release in Saliva + 0.2F solution and Saliva + pH 3.5 solution might cause cytotoxicity, but the Cu ion release in Hank's and Saliva solution (about 26 mg·L^{-1}) would not be cytotoxic. It is very necessary to investigate the in vitro cell compatibility in the next step.

5 Conclusion

In this article, the tribocorrosion behavior of Ti–Cu alloys was studied in different SBFs in comparison with cp-Ti. And the major results and conclusions were summarized as follows. Fluoride ions and the low pH value had a negative impact on corrosion and wear resistance of both Ti–Cu alloys and cp-Ti. Ti–Cu sintered alloys showed much more excellent tribocorrosion resistance than cp-Ti in all test solutions, including F ion containing and low pH solutions, due to the formation of Ti_2Cu phase. Extruded Ti–Cu alloys had much more excellent tribocorrosion property in comparison with Ti–Cu sintered alloys because of grain refinement and homogeneously distributed Ti_2Cu.

Acknowledgements This work was financially supported by the National Natural Science Foundation (No. 31971253) and Heilongjiang Provincial Basic Scientific Research Business Fund for Universities (No. 2018-KYYWF-0931).

Declarations

Conflict of interests The authors declare that they have no conflict of interest.

References

[1] Geetha M, Singh A, Asokamani R, Gogia A. Ti based biomaterials, the ultimate choice for orthopaedic implants–a review. Prog Mater Sci. 2009;54(3):397.
[2] Long M, Rack HJ. Titanium alloys in total joint replacement—a materials science perspective. Biomaterials. 1998;19(18):1621.
[3] Gepreel MA, Niinomi M. Biocompatibility of Ti-alloys for long--term implantation. J Mech Behav Biomed Mater. 2013;20:407.
[4] Watari F, Yokoyama A, Omori M, Hirai T, Kondo H, Uo M, Kawasaki T. Biocompatibility of materials and development to functionally graded implant for bio-medical application. Compos Sci Technol. 2004;64(6):893.
[5] Banerjee R, Das S, Mukhopadhyay K, Nag S, Chakrabortty A, Chaudhuri K. Involvement of in vivo induced cheY-4 gene of Vibrio cholerae in motility, early adherence to intestinal epithelial cells and regulation of virulence factors. FEBS Lett. 2002;532(1–2):221.
[6] Song Y, Xu D, Yang R, Li D, Hu Z. Theoretical investigation of ductilizing effects of alloying elements on TiAl. Intermetallics. 1988;6(3):157.
[7] Joshi MG, Advani SG, Miller F, Santare MH. Analysis of a femoral hip prosthesis designed to reduce stress shielding. J Biomech. 2000;33(12):1655.
[8] Gross S, Abel E. A finite element analysis of hollow stemmed hip prostheses as a means of reducing stress shielding of the femur. J Biomech. 2001;34(8):995.
[9] Lalor P, Revell P, Gray A, Wright S, Railton G, Freeman M. Sensitivity to titanium. A cause of implant failure? Bone Jt J. 1991;73(1):25.
[10] Olmedo D, Fernández MM, Guglielmotti MB, Cabrini RL. Macrophages related to dental implant failure. Implant Dent. 2003;12(1):75.
[11] Zhao L, Chu PK, Zhang Y, Wu Z. Antibacterial coatings on titanium implants. J Biomed Mater Res Part B Appl Biomater. 2009;91(1):470.
[12] Zheng L, Qian S, Liu XY. Induced antibacterial capability of TiO_2 coatings in visible light via nitrogen ion implantation. Trans Nonferrous Metals Soc China. 2020;30(1):171.
[13] Liu Z, Zhu Y, Liu X, Yeung KW, Wu S. Construction of poly (vinyl alcohol)/poly (lactide-glycolide acid)/vancomycin nanoparticles on titanium for enhancing the surface self-antibacterial activity and cytocompatibility. Coll Surf B Biointerfaces. 2017;151:165.
[14] Jin X, Gao L, Liu E, Yu F, Shu X, Wang H. Microstructure, corrosion and tribological and antibacterial properties of Ti–Cu coated stainless steel. J Mech Behav Biomed Mater. 2015;50:23.
[15] Wu H, Zhang X, He X, Li M, Huang X, Hang R, Tang B. Wear and corrosion resistance of anti-bacterial Ti–Cu–N coatings on titanium implants. Appl Surf Sci. 2014;317:614.
[16] Kustas F, Misra M. Friction and wear of titanium alloys. ASM Int ASM Handb. 1992;18:778.
[17] Grupp TM, Meisel HJ, Cotton JA, Schwiesau J, Fritz B, Blömer W, Jansson V. Alternative bearing materials for intervertebral disc arthroplasty. Biomaterials. 2010;31(3):523.
[18] Pina VG, Amigó V, Muñoz AI. Microstructural, electrochemical and tribo-electrochemical characterisation of titanium-copper biomedical alloys. Corros Sci. 2016;109:115.
[19] Landolt D, Mischler S, Stemp M. Electrochemical methods in tribocorrosion: a critical appraisal. Electrochim Acta. 2001; 46(24):3913.
[20] Mischler S. Triboelectrochemical techniques and interpretation methods in tribocorrosion: a comparative evaluation. Tribol Int. 2008;41(7):573.
[21] Diomidis N, Celis JP, Ponthiaux P, Wenger F. Tribocorrosion of stainless steel in sulfuric acid: identification of corrosion–wear components and effect of contact area. Wear. 2010;269(1):93.
[22] Priya R, Mallika C, Mudali UK. Wear and tribocorrosion behaviour of 304L SS, Zr-702, Zircaloy-4 and Ti-grade2. Wear. 2014;310(1):90.
[23] Watson S, Friedersdorf F, Madsen B, Cramer S. Methods of measuring wear-corrosion synergism. Wear. 1995;181:476.
[24] Jiang J, Stack M, Neville A. Modelling the tribo-corrosion interaction in aqueous sliding conditions. Tribol Int. 2002; 35(10):669.
[25] Zhang EL, Li FB, Wang HY, Liu J, Wang CM, Li MQ, Yang K. A new antibacterial titanium-copper sintered alloy: preparation and antibacterial property. Mater Sci Eng C-Mater Biol Appl. 2013;33(7):4280.
[26] Zhang EL, Li S, Ren J, Zhang L, Han Y. Effect of extrusion processing on the microstructure, mechanical properties, biocorrosion properties and antibacterial properties of Ti–Cu sintered alloys. Mater Sci Eng C. 2016;69:760.
[27] Liu J, Li F, Liu C, Wang H, Ren B, Yang K, Zhang EL. Effect of Cu content on the antibacterial activity of titanium–copper sintered alloys. Mater Sci Eng C. 2014;35:392.
[28] Zhang EL, Zheng L, Liu J, Bai B, Liu C. Influence of Cu content on the cell biocompatibility of Ti–Cu sintered alloys. Mater Sci Eng C. 2015;46:148.

[29] Zhang EL, Fu S, Wang RX, Li HX, Liu Y, Ma ZQ, Liu GK, Zhu CS, Qin GW, Chen DF. Role of Cu element in biomedical metal alloy design. Rare Met. 2019;38(6):476.
[30] Zhang EL, Zhao XT, Hu JL, Wang RX, Fu S, Qin GW. Antibacterial metals and alloys for potential biomedical implants. Bioact Mater. 2021;6(8):2569.
[31] Ren L, Ma Z, Li M, Zhang Y, Liu W, Liao Z, Yang K. Antibacterial properties of Ti–6Al–4V–*x*Cu alloys. J Mater Sci Technol. 2014;30(7):699.
[32] Zhang EL, Wang X, Chen M, Hou B. Effect of the existing form of Cu element on the mechanical properties, bio-corrosion and antibacterial properties of Ti–Cu alloys for biomedical application. Mater Sci Eng C. 2016;69:1210.
[33] Zhang EL, Li S, Ren J, Zhang L, Han Y. Effect of extrusion processing on the microstructure, mechanical properties, bio-corrosion properties and antibacterial properties of Ti–Cu sintered alloys. Mater Sci Eng C Mater Biol Appl. 2016;69:760.
[34] Teoh SH. Fatigue of biomaterials: a review. Int J Fatigue. 2000;22(10):825.
[35] Osorio WR, Freire CM, Caram R, Garcia A. The role of Cu-based intermetallics on the pitting corrosion behavior of Sn–Cu, Ti–Cu and Al–Cu alloys. Electrochim Acta. 2012;77:189.
[36] Reclaru L, Lerf R, Eschler PY, Blatter A, Meyer JM. Pitting, crevice and galvanic corrosion of REX stainless-steel/CoCr orthopedic implant material. Biomaterials. 2002;23(16):3479.
[37] Lindholm-Sethson B, Ardlin BI. Effects of pH and fluoride concentration on the corrosion of titanium. J Biomed Mater Res. 2008;86(1):149.
[38] Osório WR, Cremasco A, Andrade PN, Garcia A, Caram R. Electrochemical behavior of centrifuged cast and heat treated Ti–Cu alloys for medical applications. Electrochim Acta. 2010;55(3):759.
[39] Johnson KL. Contact mechanics and the wear of metals. Wear. 1995;190(2):162.
[40] Liu C, Zhang EL. Biocorrosion properties of antibacterial Ti–10Cu sintered alloy in several simulated biological solutions. J Mater Sci Mater Med. 2015;26(3):142.
[41] Fazel M, Salimijazi HR, Golozar MA, Jazi MR. A comparison of corrosion, tribocorrosion and electrochemical impedance properties of pure Ti and Ti6Al4V alloy treated by micro-arc oxidation process. Appl Surf Sci. 2015;324:751.
[42] Li SJ, Yang R, Li R, Hao YL, Cui YY, Niinomi M, Guo ZX. Wear characteristics of Ti–Nb–Ta–Zr and Ti–6Al–4V alloys for biomedical applications. Wear. 2004;257(9):869.
[43] Wimmer MA, Loos J, Nassutt R, Heitkemper M, Fischer A. The acting wear mechanisms on metal-on-metal hip joint bearings: in vitro results. Wear. 2001;250(1):129.